

AN OPTIMISATION PROBLEM OF HEAT APPLICATION IN SUPERSONIC FLOW AND THE UPPER LIMIT OF THE EXTERNAL COMBUSTION ENGINE EFFICIENCY

Vladimir L. Zimont and Eugenie S. Muhin

*CRS4 Research Center POLARIS, 09010 PULA (CA), Italy
Email: zimont@crs4.it, web page: <http://www.crs4.it/>*

Key words: supersonic flows, heat application optimization, external combustion engine efficiency.

Abstract. The main aim of this work is the analysis of a gasdynamic optimization problem of external heat application and estimation of the upper limit of the efficiency coefficient of the external combustion engine. For it (in contrast with the ramjet or heat engine) we have no an ideal cycle without losses as heat application is accompanied by inherent losses of the total pressure. So for estimation of the upper limit we are inevitably forced to analyse some idealized optimization problem with an inviscid formulation that takes into account this inherent loss. In the paper we analyse the optimization problem: (i) using the linear approximation valid for thin bodies and small heat applications, and (ii) in nonlinear formulation using the original concept of heat application in the jet stream with zero mass flux. Presented results demonstrate that the upper level of the efficiency coefficient is rather small, but it grows with increasing of the flight Mach number. The nonlinear data are close to the linear results for small heat applications and are lower at larger applications mainly due to additional losses in the shock wave.

1. INTRODUCTION

Heat release in the supersonic flow near aerodynamic body due to combustion (“external combustion”) generates additional lateral or longitudinal aerodynamic forces. In the former case the additional lateral forces can be used for controlling of a flying vehicle. We analyse here the latter case, when external combustion is used for reducing of the wave resistance and generate the thrust. There are many publications devoted to this problem, for example¹⁻⁸ and in the literature are discussed different applications of external combustion. For example, in the recent paper⁶ is analysed even a possibility of using of external combustion in fact as an alternative of the scramjet system (that is very difficult and expensive in realisation) for significant improvement in reusable launch vehicle (RLV) earth-to-orbit capability. So estimation of the upper level of external combustion performance is important not only from fundamental, but also applied viewpoints.

In contrast to the ramjet (as well as classical thermal engine) we cannot estimate the upper limit of external combustion efficiency using some idealized thermodynamic cycle without losses (in the ramjet theory⁹ idealized processes contains isentropic stagnation and acceleration of flow in some hypothetical inlet and nozzle, in the heat

engine it is the Carnot cycle). The reason is that generation of the longitudinal force by heat application is inevitably accompanied by losses of the total pressure that is an inherent property of external combustion. So there is no corresponding idealized thermodynamic process without losses that would be appropriate for reasonable estimation of the upper limit efficiency. That is the reason why we used for estimation of the efficiency coefficient some idealized inviscid gasdynamic optimisation problem with distributed heat application that nevertheless contains losses caused by it. We find optimal heat application as a solution of the problem, i.e. heat release is not connected with actual physico-chemical process: mixing of injected fuel and air, specific chemical kinetics, mechanisms of turbulent combustion and so on (so the term “heat application seems more appropriate). It cardinally simplifies the problem and is justified for estimation of the upper efficiency. In this paper we give the exact solution of the linear optimization problem and develop an approximate approach to a nonlinear optimization problem using an original model of heat application in the strip of flow with zero mass flux. The optimization problems were widely investigated in nonreacting aerodynamics, see books^{10,11}. In our work we generalize some known exact results of the linear theory for the case of heat application, but for estimation of the upper limit of the efficiency in the case of nonlinear formulation of the problem we use a gasdynamic model based on our original idea of heat application in the flow with “zero mass flux”. In conclusion we notice that we use for estimation of the external combustion performance the efficiency coefficient $\eta = u_\infty R / Q_\Sigma$ instead of the traditional specific impulse $I = R / m_f$ (u_∞ is the flow velocity, R is the thrust due to heat application, Q_Σ is the integral heat application per unit of time, m_f is the fuel flow rate). We see two reasons for it:

1. In our analysis there is no fuel injection and the fuel characteristics are not controlling parameter of the problem, our results in a sense are more general. But using our data it is easy to estimate the specific impulse with the formula $I = \eta H u / u_\infty$ if additionally to specify the fuel heating power Hu , i.e. I in contrast to η depends on the fuel used.
2. The efficiency coefficient η (in comparison with the specific impulse) clearly demonstrates what part of energy “works” in the external combustion engine. Additionally the velocity u_∞ is one of the main parameters controlling the performance of the external combustion and it makes the use of η more theoretically justified (in contrast to the rocket engine where the specific impulse I is the main characteristic).

2. AERODYNAMIC FORCE AT SUPERSONIC FLOW PAST A THIN SYMMETRIC PLANE BODY AT EXTERNAL HEAT APPLICATION

In this section we analyze inviscid aerodynamics of thin symmetric plane body with distributed heat application in streamlined supersonic flow (linear approximation), Fig. 1 and deduce an expression for the longitudinal force generated by this flow, Fig. 1.

2.1. Basic equations and their solution

The system of the Euler equations is the following:

$$\begin{aligned}
\partial(\rho u)/\partial x + \partial(\rho v)/\partial y &= 0 \\
\rho u \partial u/\partial x + \rho v \partial u/\partial y &= -(1/\rho) \partial p/\partial x \\
\rho u \partial v/\partial x + \rho v \partial v/\partial y &= -(1/\rho) \partial p/\partial y \\
\rho u \partial H/\partial x + \rho v \partial H/\partial y &= W(x, y) \\
p &= \rho RT
\end{aligned} \tag{1}$$

Here u and v are the velocity components, p and ρ are the pressure and density, H is the enthalpy, $W(x, y)$ describes the distributed heat application.

We first analyse the case of thin bodies and small heat application $Q_\Sigma/c_p T_\infty \ll 1$ (Q_Σ is the integral heat application $Q_\Sigma = \iint W(x, y) dx dy$) when we can linearize this set of equations using the presentation

$$p = p_\infty + p_1, \quad \rho = \rho_\infty + \rho_1, \quad T = T_\infty + T_1, \quad \rho = \rho_\infty + \rho_1, \quad u = u_\infty + u_1, \quad v = v_\infty + v_1, \tag{2}$$

where index $(_1)$ denotes small ($p_1/p_\infty \ll 1$, $u_1/u_\infty \ll 1$, $v_1/v_\infty \ll 1$, $\rho_1/\rho_\infty \ll 1$) disturbances of the flow due to the influence of the body and the heat application, index $(_\infty)$ refers to the undisturbed flow.

Inserting the expressions (2) into the set (1) and ignoring the terms of the second and higher order of magnitude we have:

$$\rho_\infty \partial u_1/\partial x + u_\infty \partial \rho_1/\partial x + \rho_\infty \partial v_1/\partial y = 0 \tag{3}$$

$$\rho_\infty u_\infty \partial u_1/\partial x = -\partial p_1/\partial x, \tag{4}$$

$$\rho_\infty u_\infty \partial v_1/\partial x = -\partial p_1/\partial y, \tag{5}$$

$$\rho_\infty u_\infty (c_p \partial T_1/\partial x + u_\infty \partial u_1/\partial x) = W(x, y). \tag{6}$$

The equation of state in the differential form after linearization is as follows:

$$\partial p_1/\partial x = T_\infty R \partial \rho_1/\partial x + \rho_\infty R \partial T_1/\partial x. \tag{7}$$

Eliminating $\partial p_1/\partial x$, $\partial \rho_1/\partial x$, $\partial T_1/\partial x$ from the Eqs. (3) - (7) we will have after simple manipulations the resulting equation:

$$(M_\infty^2 - 1) \frac{\partial(u_1/u_\infty)}{\partial x} - \frac{\partial(v_1/u_\infty)}{\partial y} = -\frac{W(x, y)}{\rho_\infty u_\infty c_p T_\infty}. \tag{8}$$

Now we show that the flow, which is described with these linear equations, is eddy-free. Eq. (4) could be integrated over x that results $\rho_\infty u_\infty u_1 = -p_1 + f(y)$, where $f(y) \equiv 0$ that follows from the boundary condition: at $x \rightarrow -\infty$ $p_1 = 0$ and $u_1 = 0$. Hence

$$\rho_\infty u_\infty u_1 = -p_1. \tag{9}$$

From Eqs. (5) and (6) it follows that $\partial u_1/\partial y - \partial v_1/\partial x = 0$, i.e. we have a potential flow with the potential Φ :

$$\Phi(x, y) = \Phi_{\infty}(x, y) + \Phi_1(x, y), \quad u_1/u_{\infty} = \partial\Phi_1/\partial x, \quad v_1/u_{\infty} = \partial\Phi_1/\partial y. \quad (10)$$

The equation (8) takes the form:

$$\frac{\partial^2 \Phi_1}{\partial x^2} - \frac{1}{\beta^2} \frac{\partial^2 \Phi_1}{\partial y^2} = -\frac{1}{\beta^2} \frac{W(x, y)}{\rho_{\infty} u_{\infty} c_p T_{\infty}} \quad (11)$$

where $\beta^2 = M_{\infty}^2 - 1$.

The equation (11) is the inhomogeneous wave equation, its solution should be reduced to a quadrature. The boundary condition on the body surface, which is described by the expression $y = h(x)$, Fig. 1, is $(v/u)|_{y=h(x)} = h'(x)$ (gas does not penetrate inside the body), or after linearization:

$$(v_1/u_{\infty})|_{y=0} = (\partial\Phi_1/\partial y)|_{y=0} = h'(x). \quad (12)$$

The solution of the equation (11) with the boundary condition (12) is a sum of two solutions: (i) the solution of the homogeneous wave equation with the boundary condition (12) and (ii) the solution of the inhomogeneous wave equation (11) with the zero boundary condition $(\partial\Phi_1/\partial y)|_{y=0} = 0$:

$$\Phi_1(x, y) = \Phi_{10}(x, y) + \Phi_{1H}(x, y). \quad (13)$$

Taking into account that the flow perturbations, which are caused by the body, travel only downstream, the solution of the homogeneous equation is as follows:

$$\Phi_{10}(x, y) = (1/\beta) h(x - \beta y). \quad (14)$$

The solution of the inhomogeneous wave equation could be deduced using the known reflection method. It is based on the fact that the boundary condition is automatically valid if we analyze the problem in all space using imaginary heat sources, which are mirrored from the wall. This solution is as follows

$$\Phi_{1H}(x, y) = \frac{1}{2\beta} \int_{-\infty}^x d\xi \int_{y-\frac{x-\xi}{\beta}}^{y+\frac{x-\xi}{\beta}} \frac{W(\xi, \eta)}{\rho_{\infty} u_{\infty} c_p T_{\infty}} d\eta. \quad (15)$$

In accordance with Eq. (10)

$$\frac{u_1}{u_{\infty}} = -\frac{h'(x - \beta y)}{\beta} - \frac{1}{2\beta^2 \rho_{\infty} u_{\infty} c_p T_{\infty}} \int_{-\infty}^x d\xi \int_{-\infty}^x [W(\xi, \frac{x-\xi}{\beta} + y) + W(\xi, \frac{\xi-x}{\beta} + y)] d\eta$$

and

$$\frac{v_1}{u_\infty} = -h'(x - \beta y) - \frac{1}{2\beta^2 \rho_\infty u_\infty c_p T_\infty} \int_{-\infty}^x d\xi \int_{-\infty}^x [W(\xi, \frac{x-\xi}{\beta} + y) - W(\xi, \frac{\xi-x}{\beta} + y)] d\eta.$$

2.2. An expression for the longitudinal aerodynamic force

In the linear approximation the pressure coefficient C_d could be written using Eq. (9) as follows:

$$C_d = \frac{2(p - p_\infty)}{\rho_\infty u_\infty^2} = \frac{2p_1}{\rho_\infty u_\infty^2} = -2 \frac{u_1}{u_\infty}$$

that after expressing the velocity in terms of the potential is the following

$$C_d = 2 \frac{h'(x)}{\beta} + \frac{2}{\beta^2} \int_{-\infty}^x \frac{W(\xi, \frac{x-\xi}{\beta})}{\rho_\infty u_\infty c_p T_\infty} d\xi. \quad (16)$$

Let us denote by $q(x^*)$ the density of the integral amount of heat releasing along the characteristic arriving to the point with the coordinate x^* (it has the angle of inclination to the axis x equal to $\gamma = \arcsin M_\infty^{-1}$), Fig.1:

$$q(x_0) = \frac{M_\infty}{\beta} \int_{-\infty}^{x_0} W(\xi, \frac{x_0-\xi}{\beta}) d\xi.$$

The amount of the heat in the space between two characteristics arriving in point x and $x + dx$ is equal to $q(x)dx/M_\infty$. The heat $Q(x)$ that is released upstream of the characteristic arriving in a point x is equal to

$$Q(x) = \frac{1}{M_\infty} \int_{-\infty}^x q(\xi) d\xi.$$

So the coefficient of the pressure on the body surface can be written as follows

$$C_d = 2 \frac{h'}{\beta} + \frac{2}{\beta} \frac{q(x)}{M_\infty \rho_\infty u_\infty c_p T_\infty} = 2 \frac{h'(x)}{\beta} + \frac{2}{\beta} \frac{Q'(x)}{\rho_\infty u_\infty c_p T_\infty}. \quad (17)$$

It means that the peculiarity of the solution of the linearized equations is that the pressure in a point on the body surface is controlled only by the integral amount of the heat, which is released on the characteristic arriving in this point, and does not depend on the distribution of the heat application along the characteristic. The final result is that the drag (or thrust depending on the sign) R_x of the body is equal to

$$R_x = \frac{\rho_\infty u_\infty^2}{2} \int_{x_{ii}}^{x_f} C_d h'(x) dx$$

or taking into account the expression (17) it can be presented as follows:

$$R_x = \frac{\rho_\infty u_\infty^2}{2} \int_{x_i}^{x_f} (h'^2(x) dx + \frac{Q'(x)h'(x)}{\rho_\infty u_\infty c_p T_\infty}) dx \quad (18)$$

In Eq. (18) x_i and x_f are initial and final coordinates of the body, Fig. 1.

3. THE BODY PROFILE OPTIMIZATION AT GIVEN HEAT APPLICATION

Actual heat application, which takes place due to combustion at injection of fuel into the air flow, is controlled by several physical-chemical processes: molecular-turbulent mixing, chemical kinetics of used fuel, mechanisms of turbulent combustion. In this section we assume that heat application is known and it does not depend on the body profile, i. e. we assume that the given function $Q(x)$ is fixed at the body profile variations and known. This assumption is theoretically justified for thin profiles. The optimization problem formulation is the following: to find the profile $h(x)$ yielding the minimal wave resistance.

3.1. Formulation of the problem and equations

In this problem we assume that the heat application could be also upstream of the body. We introduce the characteristic length L_q where takes place complete heat application, i.e. the function $Q(x)$ can be presented as follows:

$$Q(x) = \begin{cases} 0, & x < x_q, \\ \tilde{Q}(x), & x_q \leq x \leq x_q + L_q, \\ 0, & x > x_q + L_q. \end{cases} \quad (19)$$

In this problem we allow that heat application can be also upstream of the body and in the general case takes into account wall friction.

The drag of the body per unit of the body width is the following

$$R_x = \frac{\rho_\infty u_\infty^2}{\beta} \int_{x_{ii}}^{x_f} (h'(x) + \frac{Q'(x)h'(x)}{\rho_\infty u_\infty c_p T_\infty} + C_f) dx \quad (20)$$

where C_f is the coefficient of resistance that is assumed to be constant.

Formulation of the problem is the following: between functions $h(x)$ describing the profile of a body with fixed length $x_f - x_i = L$ and boundary conditions on the beginning and the end of the body $h(x_i) = h(x_f) = 0$ we must find such profile that minimize the integral in Eq. (20) where $Q(x)$ is described by Eq. (19). The body can have additional restriction such as the maximal thickness H and the area S :

$$S = \int_{x_i}^{x_f} h(x) dx. \quad (21)$$

This problem with the isoperimetric condition (21) is equivalent to defining the extreme of the functional

$$R_x = \frac{\rho_\infty u_\infty^2}{\beta} \int_{x_i}^{x_f} F dx \quad (22)$$

where $F = h'^2(x) + \frac{Q'(x)h'(x)}{\rho_\infty u_\infty c_p T_\infty} + C_f + \lambda h'(x)$ where λ is the Lagrange multiplier.

The Euler equation of the optimization problem in this case is the following:

$$\lambda - 2h''(x) + \frac{Q''(x)}{2\rho_\infty u_\infty c_p T_\infty} = 0$$

and hence after integration

$$h(x) = -\frac{Q(x)}{2\rho_\infty u_\infty c_p T_\infty} - \frac{\lambda x^2}{4} + ax + b, \quad (23)$$

where a and b are constants that is defined from the boundary conditions.

In the general case the optimal profile $h(x)$ consists of several arcs described by Eq. (23). The conditions in the junction points are the following:

$$\Delta[-h'^2(x) + \lambda h(x)]\delta x + \Delta[2h'(x) + \frac{Q'(x)}{\rho_\infty u_\infty c_p T_\infty}]\delta h = 0$$

where the symbol Δ denotes the difference between the values in brackets corresponding to the left and right sides of the angular point. If there is no any restrictions on the angular points coordinates we have in this case that

$$\Delta[h'^2(x)] = 0, \quad \Delta[2h'(x) + \frac{Q'(x)}{\rho_\infty u_\infty c_p T_\infty}] = 0. \quad (24)$$

If the given thickness of the body is achieved in a junction point it would be sufficient to put the condition

$$\Delta[h'^2(x)] = 0. \quad (25)$$

And at last in the case when there are variations of the coordinates of the beginning and the end of the body with respect to the zone of heat application, the transversability condition must be valid. As we assumed that $h(x_i) = h(x_f) = 0$ the transversability condition is the following:

$$[-h'^2(x_i) + C_f] \delta x_i - [-h'^2(x_f)] \delta x_f = 0. \quad (26)$$

The Lagrange multiplier λ is found from the isoperimetric condition (21).

3.2. Optimal profiles and drag in the case $Q(x) = 0$ (without heat application)

We analyze first the optimal profile of the body without external heat application and we will compare the aerodynamic drag of this body with the drag of the optimal body with heat application. For given length and thickness of the body we will analyze particular cases corresponding to different values of the area S of the isoperimetric condition. It is more convenient to set the value of the Lagrange multiplier λ or the geometric parameters of the body and to define corresponding values of the area, the body profile and corresponding drag.

a) Let $C_f = 0$ and $\lambda = 0$, the length of the body L and the thickness H are given.

In this case in accordance with (23) the profile consists of straight lines. From the transversability condition (26) (as at $L = const$ $\delta x_i = \delta x_f$) it follows that

$[h'(x_i)]^2 = [h'(x_f)]^2$ and the optimal body in this case is the rhomb with given thickness in the middle of the chord, with the area of the cross section $S = 0.5LH$

and with the wave resistance $R_x = \frac{\rho_\infty u_\infty^2}{\sqrt{M_\infty^2 - 1}} \frac{H^2}{L}$.

b) Let us choose such value of λ that in the section with maximum thickness the profile would have zero derivative, i. e. in the section with $h_{\max} = H/2$ $dh/dx = 0$.

In this case the optimal profile is described by one curve of the second order (23) and taking into account (26) we have

$$h(x) = 2H \frac{x}{L} \left(1 - \frac{x}{L}\right), \quad \lambda = \frac{8H}{L^2}, \quad S = \frac{2}{3}HL, \quad R_x = \frac{4}{3} \frac{\rho_\infty u_\infty^2}{\sqrt{M_\infty^2 - 1}} \frac{H^2}{L}.$$

This smooth profile has the area and the drag that is 4/3 times larger than has the body with rhomb profile.

c) In the case $-\infty < \lambda < -\frac{8H}{L^2}$ the optimal body consists of the arcs 1-2, 3-4 and the straight line 2-3, and in accordance with (25) in the points 2 and 3 there is no break, i. e. there is no the derivative discontinuity of $h'(x)$. If point 2 has the coordinate 0.5ξ where $\xi \ll 1$ the optimal body is described by the formulas (the body is

$$\text{symmetrical by } x = 0.5L): \quad h(x) = \begin{cases} 2H \frac{x}{\xi L} \left(1 - \frac{x}{\xi L}\right), & 0 \leq x \leq 0.5\xi \\ \frac{H}{2}, & 0.5\xi \leq x \leq 0.5 \end{cases}$$

$$\text{and here } \lambda = \frac{8H}{\xi^2 L^2}, \quad S = \left(1 - \frac{\xi}{3}\right)HL, \quad R_x = \frac{4}{3\xi} \frac{\rho_\infty u_\infty^2}{\sqrt{M_\infty^2 - 1}} \frac{H^2}{L}.$$

In the case $\xi \rightarrow 0$ the optimal body tend to the rectangle with the sides H and L (i. e. $S \rightarrow HL$) and $R_x \rightarrow \infty$. It is obvious that this limiting case is purely formal as the linearized theory is not valid here.

d) $\lambda > 0$ and $S < 0.5HL$. It is easy to check that in this case

$$h(x) = \frac{\lambda x^2}{4} + \left(\frac{H}{L} - \frac{\lambda L}{8}\right)x, \quad 0 \leq x \leq \frac{1}{2},$$

$$S = \frac{HL}{2} - \lambda \frac{L^3}{48}, \quad R_x = \frac{\rho_\infty u_\infty^2}{\sqrt{M_\infty^2 - 1}} \left(\frac{\lambda^2 L^3}{192} + \frac{H^2}{L} \right).$$

We have from the condition $h(x) \geq 0$ that the maximal possible value λ is equal to $\lambda = 8H/L$. For this value $dh/dx = 0$ in the points $x = 0$ and $x = L$ and $dh/dx = 2H/L$ in the point $x = 1/2$. In this case the area is $S = HL/3$ that is the minimal possible value and the drag of such concave body is equal to the drag of the convex body with smooth profile in the section where the thickness is maximal. In the case $\lambda > 8H/L^2$ the degenerated case takes place when between points 1-2 and 4-5 the thickness is equal to zero, i. e. at the area $S < HL/3$ the length of the optimal profile in fact is reduced and it is situated between the points 2 and 4 so the linearized theory is not valid as in accordance with the recommendations from the literature¹¹ the linearized theory is valid when $H/L < 0.1$.

e) The particular solutions from the items a)-d) are the classical solutions of the theory of optimal aerodynamics forms¹¹. At fixed length of the optimal body, the profile does not depend on friction. But without restriction on the body length it is controlled directly by the coefficient of restriction C_f . In the literature there are such solutions for the bodies with fixed thickness and the area of the cross-section.

3.3. Effect of heat application and optimal profiles for different $Q(x)$.

Now we analyze the case of external combustion. Sequence and number of arcs described by Eq. (23) and constituting the optimal profile depend on coordinates of beginning and end of the heat application x_q and $x_q + L_q$ as well as by coordinate x_0 where the body has the maximum thickness $h(x_0) = h_{\max} = H/2$. From Eq. (24) written for the angular point x_q for the cases $x_q > x_0$ or $x_q < x_0$ follows that $Q'(x_q) = 0$ and $h_2'(x_q) = h_1'(x_q)$. A similar situation takes place in the angular point $x_q + L_q$. But in the case $Q'(x_q) \neq 0$ in accordance with Eq. (25) beginning of heat application can be only in the section $x_q = x_0$ with the maximal width. Finally the possible optimal configuration consists of two arcs $h_1(x)$ and $h_2(x)$ corresponding to Eq. (23) and containing one angular point in $x = x_0$. Now we take a look at the case when $Q'(x_q) = Q'(x_q + L_q) = 0$ that corresponds to physically reasonable case of smooth beginning in $x = x_q$ and smooth extinguish in $x = x_q + L_q$ of combustion. From the set of equations (27) we can find corresponding to this case unknown x_0 , x_i and x_f and after this Eq. (22) gives the value of the minimal drag of the optimal body.

$$\begin{cases} h_1(x_i) = 0, & h_1'(x_i) = \sqrt{C_f}, & h_2(x_f) = 0, & h_2'(x_f) = \sqrt{C_f}, \\ h_1(x_0) = H, & h_2(x_0) = H, & h_1''(x_0) = h_2''(x_0), & S = \int_{x_i}^{x_f} h(x) dx. \end{cases} \quad (27)$$

Fig. 2 demonstrates optimal configurations corresponding to different cases:

- a. heat application begins upstream from the section of the maximum thickness;
- b. heat application takes place on the back side (stern) of the body;
- c. heat application begins in the section of maximal thickness of the body.

In conclusion we give several examples that illustrate the effect of external heat application on the drag showing the ratio R_x^Q/R_x where R_x^Q and R_x correspond to different optimal bodies with and without external heat application, but with the same length and maximal width. In all examples we assumed that $Q_\Sigma = \rho u_\infty c_p T_\infty H$ where Q_Σ is the summary amount of heat released in all space in a unit time ($Q(x) \leq Q_\Sigma$). Figs. 3A-3C demonstrate profiles of the optimal bodies in the cases different functions of heat application $Q(x)$ together with corresponding values of the ratio R_x^Q/R_x . Every figure present two cases: (a) when the body length and the extent of the heat application are equal $L_q/L=1$ and (b) the latter is much shorter $L_q/L=1/4$. We analyzed linear function $Q(x) \sim (x-x_q)/L_q$ (Fig. 3A) and two parabolic distributions $Q(x)$ with different signs of the curvature: $Q(x) \sim (x-x_q)^2/L_q^2$ and $Q(x) \sim (x-x_q)(2L_q-x+x_q)/L_q^2$ (Fig. 3B and Fig. 3C). It is interesting to note that in the case $L_q/L=1$ at positive curvature, Fig. 3B(a) all heat is used for reduction of the drag while at negative curvature, Fig. 3C(a) only part of it. We see that the curvature sign of $Q(x)$ qualitatively influence on the optimal body profile.

Results presents in Figs. 3 do not depend on the Mach number $M_\infty > 1$. For validity of the linear approximation first the body width must be relatively thin $H/L \ll 1$ and (ii) the body length must be sufficiently long to satisfy the condition of small intensity of heat application $\alpha = (\rho u_\infty c_p T_\infty)^{-1} dQ/dx \ll 1$ as $\alpha \sim Q_\Sigma/L$. So in the context of the linear approximation we can increase Q_Σ and L keeping $H/L = const$ and at sufficiently large heat application we will have the thrust instead of the drag. We here do not analyze the corresponding efficiency coefficient as its value does not present the upper limit of the coefficient following from the variational problem, which optimize both the body profile and the heat application.

4. OPTIMIZATION OF THE BODY PROFILE AND HEAT APPLICATION AND THE UPPER LIMIT OF THE EXTERNAL COMBUSTION EFFICIENCY

It is obvious that for estimation of the maximal potentiality of external combustion we must optimize both the body profile and heat application. In this section we analyse this problem in linear approximation, the last section is devote to a nonlinear formulation.

4.1. Upper limit of the external combustion efficiency. Formulation of the problem

Our aim was not to solve the variational problem taking into account properties of viscous turbulent gasdynamics and actual physico-chemical mechanisms controlling aerodynamic resistance and heat application, but to estimate an upper limit of the external combustion efficiency. As it was mentioned in the introduction in the case of external combustion we have no (in contrast to the standard ramjet and heat engine) appropriate ideal cycle, which would be appropriate for estimation of upper limit of the efficiency coefficient and it forces us to formulate and solve some optimisation

problem. For estimation of the upper limit of the efficiency we chose an idealized variational problem, which exclude all aerodynamic resistance and losses that are not connected with external heat application. So we analyse the configuration shown in Fig.4, where the heat application takes place only over the stern (the back part) of the body, and do not take into account the aerodynamic impedance of the front part of the body and viscous friction. We optimize both the profile of the stern and distribution of heat application $Q(x)$ using as a target function the maximal thrust and believe that this formulation of the problem is adequate to the aim of the study.

In our analysis we do not connect the volume heat application with some particular mechanism, our results are more general. It is one of the reason why we express them in terms of the efficiency coefficient $\eta = u_\infty R / Q_\Sigma$ instead of the traditionally used specific impulse $I = R / m_f$ (R is the thrust due to heat application Q_Σ , m_f is the fuel flow rate). Obviously, we can present our results in terms of the specific impulse with the formula $I = \eta H u / u_\infty$, but for this we must specify additionally the fuel heating power Hu . We notice that our variational problem does not include gasdynamic effects due to fuel injection. But keeping in mind that the stoichiometric coefficients of actual fuels are large and hence the fuel flow rate is relatively small, we can apply our estimation to the case of external combustion. But there is another argument to the benefit of using the efficiency coefficient for engineering estimations: it clearly demonstrates what part of heat energy is used in the external combustion engine.

4.2. Analysis of the variational problem

In accordance with the expression (18) the longitudinal force is controlled by the profile $y = h(x)$ and heat application $Q(x)$. It is natural to introduce a limit on the value of the maximal heat application intensity $\alpha \leq \alpha_{\max} = (\rho_\infty u_\infty c_p T_\infty)^{-1} (dQ/dx)_{\max}$. In our case this limit is defined by the condition of applicability of the linearized theory $\alpha_{\max} \ll 1$. We assume that the beginning of heat application takes place at the beginning of the back part (the stern profile) of the body, Fig. 4. We formulate the optimization problem as it follows, namely, to find such two functions: (i) $Q(x)$ describing the heat application that satisfy the condition $0 \leq Q' \leq Q'_{\max}$ and (ii) $h(x)$ describing the profile of the back part of the body with boundary conditions in $x_i = 0$ and $h(x_f) = 0$, which yield maximal efficiency coefficient $\eta = R_x u_\infty / Q_\Sigma$ (Q_Σ is the summary amount of heat released in all space in a unit time). It is significant to stress that we do not assume any additional limitation (the body thickness, volume and so on) as they could only reduce this coefficient η .

The condition $0 \leq Q' \leq Q'_{\max}$ is equivalent to the equation

$$Q'(x)(Q'_{\max} - Q'(x)) = f^2(x) \quad (28)$$

where $f(x)$ is a new real-valued function. So the problem of maximization of the functional (27) with the differential condition (28) is reduced to maximization of the functional

$$I = \int_{x_i}^{x_f} F dx \text{ with } F = [h'(x)]^2 + \frac{Q'(x)h'(x)}{\rho_\infty u_\infty c_p T_\infty} + \mu(x)[Q'(x)(Q'_{\max} - Q'(x)) - f^2(x)] \quad (29)$$

where $\mu(x)$ is the Lagrange multiplier. Optimal functions $h(x)$, $Q(x)$ and $f(x)$ are defined from the Euler equation of the variational problem:

$$F_h - \frac{d}{dx} F_{h'} = 0, \quad F_Q - \frac{d}{dx} F_{Q'} = 0, \quad F_f = 0,$$

which taking into account (20) have the form:

$$2h''(x) + \frac{Q'(x)}{\rho_\infty u_\infty c_p T_\infty} = 0, \quad (30)$$

$$\frac{h''(x)}{\rho_\infty u_\infty c_p T_\infty} + \frac{d}{dx} [\mu(x)(Q'_{\max} - 2Q'(x))] = 0, \quad (31)$$

$$\mu f = 0. \quad (32)$$

From Eq. (32) it follows that the function $Q(x)$ consists of the arcs corresponding to $\mu = 0$ and $f = 0$. Along the former arc with $\mu = 0$ is valid the strict inequality $0 < Q'(x) < Q'_{\max}$. From Eq. (32) it follows that $h' = const$ and from Eq. (30) it follows that $Q'(x) = const$. Along the arc $f = 0$ either $Q'(x) = 0$, or $Q'(x) = Q'_{\max}$. In this case from Eq. (30) it follows that here also $h'(x) = const$. So the optimal function $Q(x)$ consists in the linear distributions $Q'(x)$ and the optimal profile consist of the straight lines $h'(x) = const$. The conditions in the points of junction are the following:

$$\begin{aligned} \Delta[F - h'F_{h'} - Q'F_{Q'}] \delta x + \Delta F_{h'} \delta h + \Delta F_{Q'} \delta Q + \Delta F_f \delta f &= 0, \\ \Delta[h'^2(x) + \frac{Q'(x)h'(x)}{\rho_\infty u_\infty c_p T_\infty} - \mu(x)Q'^2(x)] \delta x + \Delta[2h'(x) + \frac{Q'(x)}{\rho_\infty u_\infty c_p T_\infty}] \delta h + \\ \Delta[\frac{h'(x)}{\rho_\infty u_\infty c_p T_\infty} + \mu(x)(Q'_{\max} - 2Q'(x))] \delta Q &= 0, \end{aligned}$$

where the symbol Δ denotes the difference between the values to the left and right of the point of break, δx , δh , δQ are arbitrary variations of the angular point coordinate and the value of $Q(x)$ in this point. For arbitrary angular point (as we do not impose any limitation on its coordinates) the latter equation is equivalent to the set of equations:

$$\Delta[h'^2(x) + \frac{Q'(x)h'(x)}{\rho_\infty u_\infty c_p T_\infty} - \mu(x)Q'^2(x)] = 0,$$

$$\Delta[2h'(x) + \frac{Q'(x)}{\rho_\infty u_\infty c_p T_\infty}] = 0,$$

$$\Delta[\frac{h'(x)}{\rho_\infty u_\infty c_p T_\infty} + \mu(x)(Q'_{\max} - 2Q'(x))] = 0.$$

Hence it follows that $\Delta h' = 0$ and $\Delta Q = 0$, i. e. angular points are impossible and the optimal heat application has constant intensity $Q' = const$.

And lastly, if takes place variations of x_i and x_f (the coordinates of the initial and final sections of the sternpost of the body) the transversability condition must be fulfilled:

$$[(F - h'F_{h'} - Q'F_{Q'})\delta x + F_{h'}\delta h + F_{Q'}\delta Q]_i^f = 0.$$

This condition written for arbitrary variations of $h(x_i)$, x_f and $Q(x_f)$ has the form

$$h'^2(x) + \frac{Q'(x)h'(x)}{\rho_\infty u_\infty c_p T_\infty} - \mu(x)Q'^2(x) = 0,$$

$$2h'(x) + \frac{Q'(x)}{\rho_\infty u_\infty c_p T_\infty} = 0,$$

$$\frac{h'(x)}{\rho_\infty u_\infty c_p T_\infty} + \mu(x)(Q'_{\max} - 2Q'(x)) = 0,$$

where h' and Q' describe the optimal inclination of the stern profile and the optimal heat application intensity. The first two equations define the Lagrange multiplier $\mu = -0.5\rho_\infty u_\infty c_p T_\infty$. Then from the last equation it follows that $Q' = Q'_{\max}$,

$h' = \frac{Q'_{\max}}{2\rho_\infty u_\infty c_p T_\infty}$. The optimal height of the body (stern) is controlled by the

integral heat application $H = \frac{Q_\Sigma}{2\rho_\infty u_\infty c_p T_\infty}$ and the maximal efficiency coefficient

depends on the gas adiabatic exponent $\kappa = c_p / c_v$:

$$\eta = (\kappa - 1) \frac{M_\infty^2}{\sqrt{M_\infty^2 - 1}} \frac{\alpha_{\max}}{4}. \quad (33)$$

Eq. (33) presents also the similarity criterion: two bodies that are flowed over by gases with different adiabatic exponents and Mach numbers have the same coefficient of efficiency when

$$(\kappa_1 - 1) \frac{M_1^2}{\sqrt{M_1^2 - 1}} \alpha_{\max}^1 = (\kappa_2 - 1) \frac{M_2^2}{\sqrt{M_2^2 - 1}} \alpha_{\max}^2.$$

Fig. 5 demonstrates values of η as a function of the maximum heat application intensities α_{\max} for different flow Mach numbers M_∞ ($\kappa = 1.4$).

Our analysis demonstrates that even the optimal body has the wave resistance and some part of the heat is used to overcome it. The wave resistance of the optimal body is equal to

$$R_x = \frac{\rho_\infty u_\infty^2}{\sqrt{M_\infty^2 - 1}} \frac{\alpha_{\max}}{4} L \quad (34)$$

(here $L = x_f - x_i$ is the length of the stern) that is half the force connected with heat application. Without heat application minimal wave resistance is equal to zero and

corresponding optimal body has zero high (the infinitely thin plate), or it is the Buzeman biplane. So for the Buzeman biplane our estimation of the efficiency coefficient gives a two times larger value.

5. NONLINEAR FORMULATION OF THE PROBLEM AND A MODEL OF HEAT APPLICATION IN THE JET STRAM WITH ZERO MASS FLUX

Our previous results refer to the linear formulation of the problem that is valid in the case of small heat application $\alpha = dQ / \rho_\infty u_\infty c_p T_\infty dx \ll 1$. For an estimation of the efficiency coefficient η , when the linearized theory is not valid, we analyze the flow over the body taking into account strong distortions and generate the shock wave by combustion. We take the profile of the body and the heat application law from the linearized solution of the optimization problem. We will analyze the flow shown in Fig. 6 where the heat application is accompanied by formation of the shock wave. We analyse this gasdynamic flow using for an estimation of the upper limit of the efficiency coefficient η an original idea in which the heat application takes place at constant pressure in a one-dimensional flow with “zero mass flux”.

5.1. A concept of heat application in the flow with “zero mass flux”

Now we present equations and give an explanation of the “zero mass flux” concept used for an estimation the upper limit of η . Let us consider the one-dimensional flow with variable cross section and heat application. It is describe by a set of equations:

$$dm = d(\rho u F) = 0, \quad dI = p dF, \quad md(c_p T + u^2 / 2) = dQ(x). \quad (35)$$

Here m and I are the mass and impulse fluxes, F is the flow area. When $p(x) = const$ Eqs. (35) results in $u(x) = const$, i. e. at isobaric heat application the one-dimensional flow velocity is constant. Simple manipulations yield for this case following expression:

$$F(x) = F_0 + \frac{\kappa - 1}{\kappa p u} Q(x), \quad (36)$$

which shows that area of the one-dimensional flow is controlled by heat application (F_0 is the jet stream area at beginning of heat application and $k = c_p / c_v$). In the limiting case $F_0 \rightarrow 0$ and the mass flux $m \rightarrow 0$ (the flow with “zero mass flux”). If we additionally assume that heat application has constant intensity $Q'(x) = const$, we have from Eq. (36) that $F(x) \sim x$. It means that in analyzed case of the plane flow and constant heat application intensity the boundary between cold and hot gases is the straight line, Fig. 6. The inclination angle of steam line. The algebraic expression for the inclination angle of streamline of the zero mass flux flow with respect to a surface of the stern is as follows:

$$tg \varphi = \frac{\kappa - 1}{\kappa p u} \frac{dQ}{dx}, \quad \text{or} \quad \alpha = \frac{p}{p_\infty} \frac{u}{u_\infty} tg \varphi, \quad \text{where} \quad \alpha = \frac{1}{\rho_\infty u_\infty c_p T_\infty} \frac{dQ}{dx}. \quad (37)$$

Taking into account Eqs. (37) the expression for the efficiency coefficient for the

configuration presented on the Fig. 6 is the following:

$$\eta = \frac{(p(\beta)/p_\infty - 1)H}{Q} u_\infty = \frac{\kappa - 1}{\kappa} \frac{(p(\beta)/p_\infty - 1)H}{\alpha} \frac{\sin \omega}{\cos((\omega + \beta)/2)}, \quad (38)$$

where H is the height of the body, β is the deviation angle of the flow behind the shock wave, the pressure p and the flow velocity u are controlled by the shock wave, the angle of the shock wave depends on the heat application intensity α .

5.2. Numerical examples

The geometrical parameters, which result in the maximal value η , were found numerically for given values α . In calculations we assumed that the gas adiabatic exponent is equal to $k = c_p/c_v = 1.4$. Fig. 7 demonstrates that at small heat applications the linear theory and nonlinear calculations are close. Fig. 8 presents the optimal dimensionless height $\bar{H} = H/L$ as a function of α . Figs. 9 - 11 show nonlinear results for η corresponding to different Mach numbers of the flow M_∞ (for comparison Fig. 9 contains also the result of the linearized theory). The maximal values of η (and maximal heat application) correspond to limiting condition of the flow with the attached shock. Fig. 12 shows η as a function of the flow Max number M_∞ . It is probably significant for application to note that at least in principle the efficiency of external combustion increases when the flight Max number grows.

Presented relatively low levels of the upper limit of the efficiency coefficient indicate that engineering analyse of the external combustion engine practicability needs very accurate numerical simulations (and, obviously, experimental validations). Keeping in mind this moment we believe that our theoretical results have not only a fundamental value, but also could be of practical use for more realistic understanding of the external combustion potentiality, which sometimes (especially in past) was overestimated due to the absence of the upper limit estimations. And though we do not investigate a problem of feasibility of the external combustion engine (the aim was to analyse a more fundamental aspect of external combustion) in accordance with our intuitive understanding of this concept, we believe that the external combustion engine will find some practical application.

6. CONCLUSIONS

1. We formulated and resolved the optimization problem of external heat application in the linearized formulation, which is valid for thin aerodynamic bodies and small heat applications, for the plane symmetrical aerodynamic body at supersonic flow velocities. We analyzed two isoperimetric variational problems using the method of Lagrange multipliers and found (i) the optimal body profiles at given function of the heat application $Q(x)$ and (ii) both optimal body profile $h(x)$ and optimal heat application $Q(x)$, which yield the upper limit of the efficiency coefficient η .
2. We analyze the nonlinear optimization problem in the context of a gasdynamic scheme, which follows from the solution of the liner variational problem, and apply an original model of the heat application in the flow with zero mass flux.

3. We interpret our results in term of upper limit of the efficiency coefficient of the external combustion used for generation of the jet thrust. Presented numerical results demonstrate that for small heat applications linear and non-linear formulations of the problem give close results but at larger heat applications the efficiency becomes significantly lower in the case of nonlinear formulation.
4. We believe that estimation of the upper limit of supersonic burning performance has not only fundamental but also applied importance in the frame of the concept of the external combustion engine aimed for possible applications in the aero-space systems (in particular for perspective earth-to-orbit reusable launch vehicle) and in the hypersonic aircraft.

7. REFERENCES

- [1] F.S. Billig, "External Burning in Supersonic Streams", *The Johns Hopkins University Appl. Phys. Lab. Memor.*, (1967).
- [2] E.A.Fletcher, R.G. Dorsch, H. Allen, "Combustion of Highly Reactive Fuels in Supersonic Airstreams", *ARS Journal*, IV, v. 30, No. 4, (1960).
- [3] E.G. Broadbent, "Flows with heat addition", *Progress in Aerospace Science*, v. 17, N. 2, 93-108 (1976).
- [4] V.S. Sadovsky and G.I. Taganov, *About a generate flow of supersonic flow with heat application and flow angularity*, Proceedings of TsAGI, issue 1157 (1969), (in Russian).
- [5] F.S. Billig, "Research on supersonic combustion", *Journal of Propulsion and Power*, vol. 9, No. 4, 499-514 (1993).
- [6] H. Froning, and R. Roach, "Investigation of Hypersonic Drag Reduction and Thrust Increase by External Burning", AIAA-2003-6906, *12th AIAA International Space Planes and Hypersonic Systems and Technologies* (2003).
- [7] S. Coras, and A. Paull. Experiments on External Combustion with Leading Edge Fuel-Injection in Hypersonic Flow", AIAA Paper AIAA-2006-7981, *14th AIAA/AHI Space Planes and Hypersonic Systems and Technologies Conference* (2006).
- [8] John W. Hicks, "Development of a Hydrogen External Burning Flight Test Experiment on the Nasa Dryden SR-71a Aircraft", *SAE Technical Papers*, No. 920997 (2007)
- [9] V.S. Zuev, and V.S. Makaron, *Theory of Air-Breathing Engines and Rocket Scramjets*, Mashinostroenie, Moscow (1971) (in Russian).
- [10] A. Miele (editor), *Theory of Optimum Aerodynamic Shapes*, Academic Press, New York (1965).
- [11] A.N. Kraiko, *Variational Problems of Gas Dynamics*, 1979 - Nauka, Moscow (1979) (in Russian).

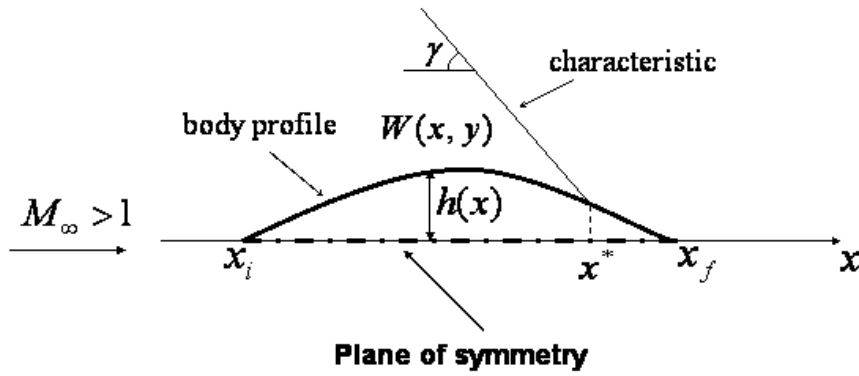


Fig. 1. Illustration to the linearized problem.

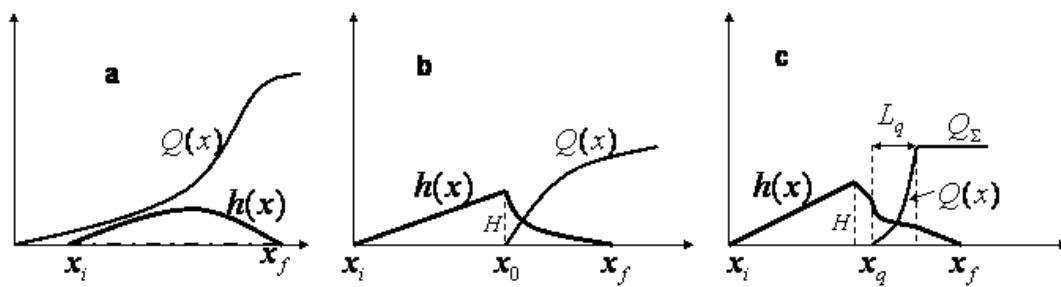


Fig. 2. Configurations of optimal body profiles $h(x)$ at different heat applications $Q(x)$.

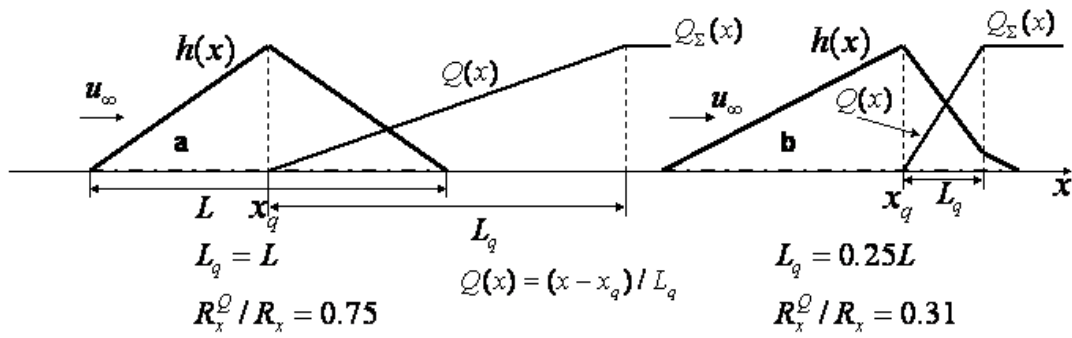


Fig. 3A. The drag reduction and optimal profiles at linear heat application $Q(x)$.

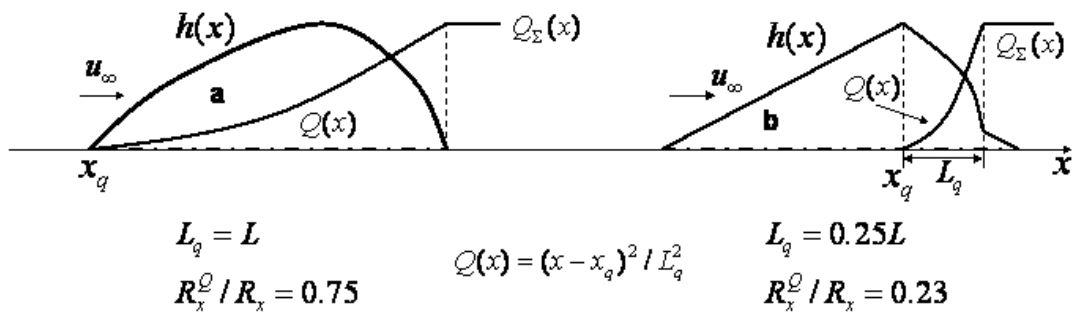


Fig. 3B. The drag reduction and profiles at parabolic $Q(x)$ with positive curvature.

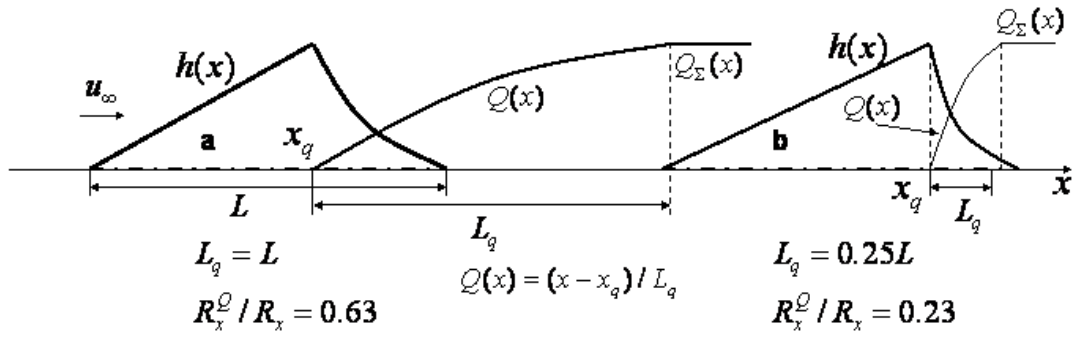


Fig. 3C. The drag reduction and profiles at parabolic $Q(x)$ with negative curvature.

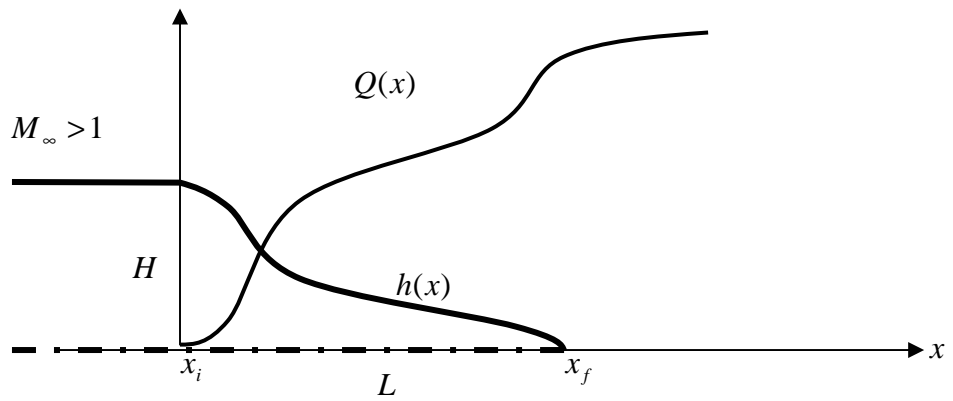


Fig.4. The body configuration to the problem of estimation of the upper limit efficiency.

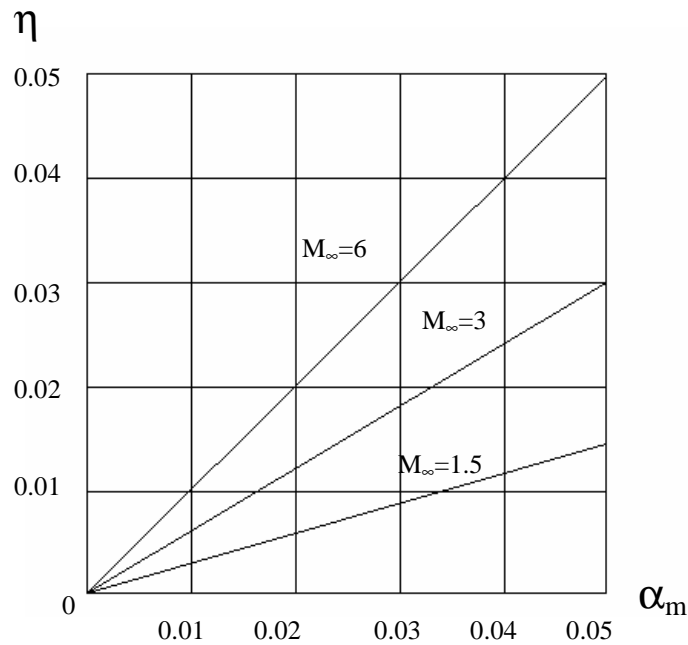


Fig.5. The upper limit of the efficiency coefficient in the context of the linear optimization problem, α_m is the maximal heat application intensity.

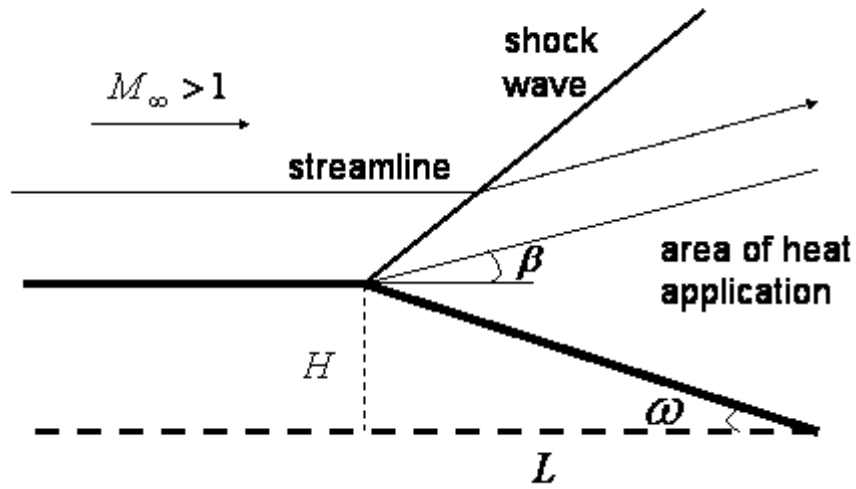


Fig. 6. Gasdynamic scheme for nonlinear formulation of the problem.

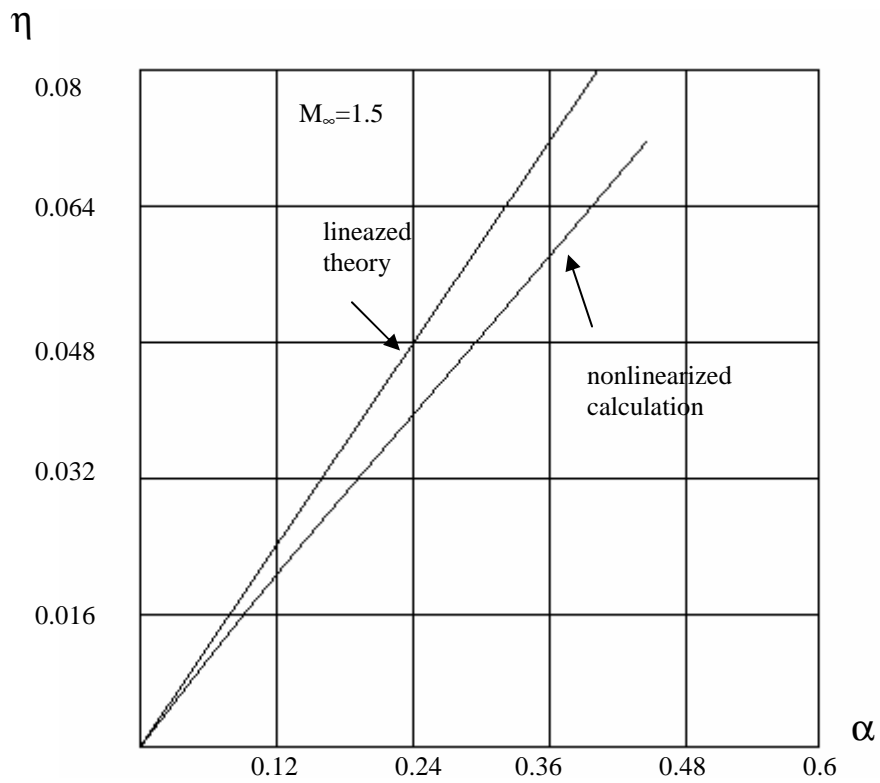


Fig.7. The efficiency in the context of the linear theory and nonlinear calculation.

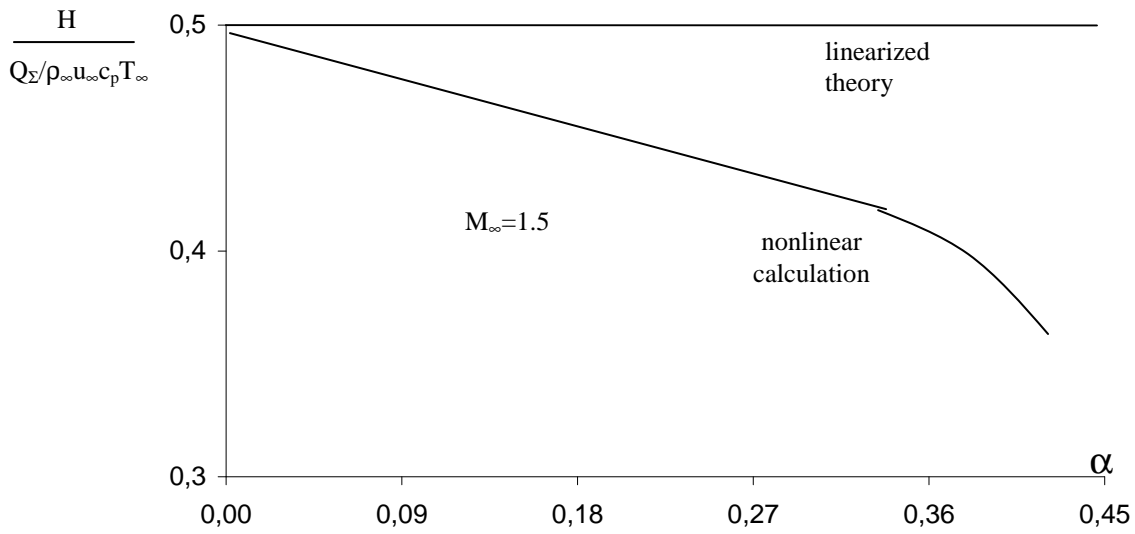


Fig. 8. Dependence of the width of the optimal body on summary heat application,

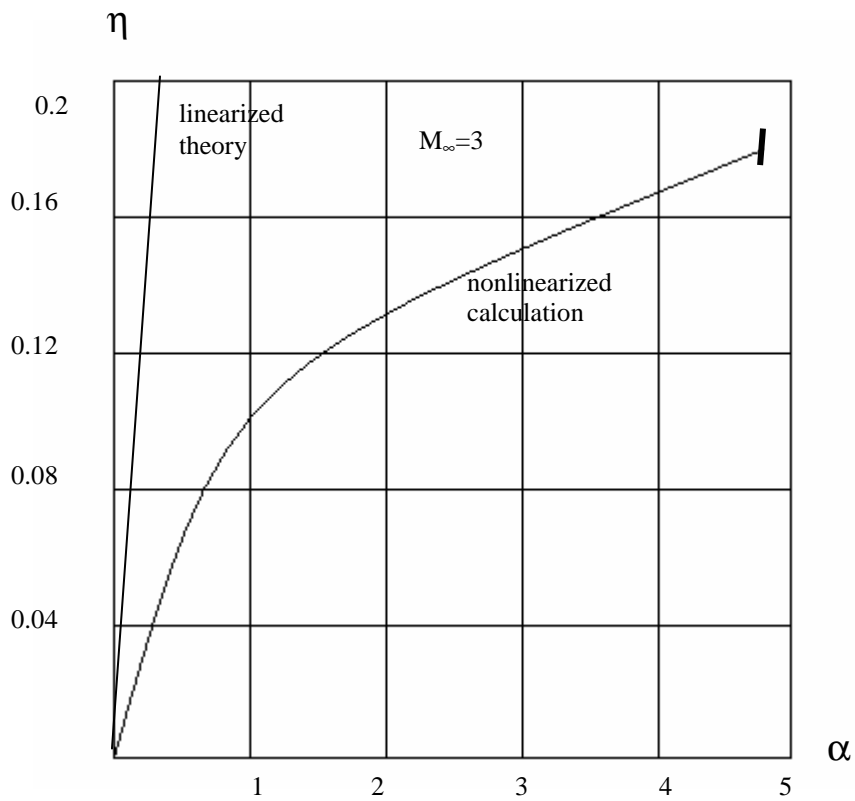


Fig.9. Dependence of the upper limit of the efficiency coefficient on the heat application intensity, nonlinear calculation, $M_\infty = 3$.

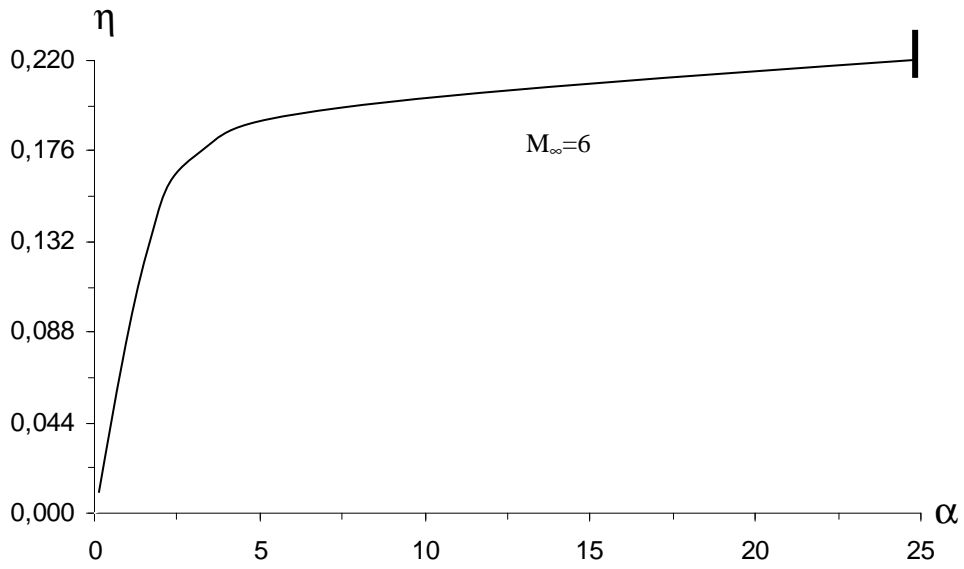


Fig.10. Dependence of the upper limit of the efficiency coefficient on the heat application intensity, nonlinear calculation, $M_\infty = 6$.

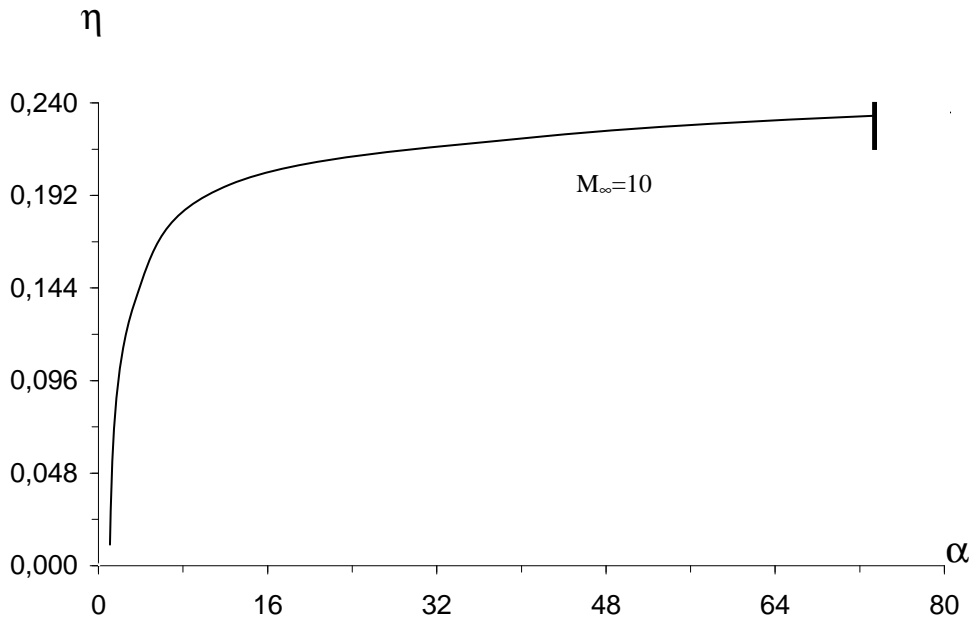


Fig.11. Dependence of the upper limit of the efficiency coefficient on the heat application intensity, nonlinear calculation, $M_\infty = 10$.

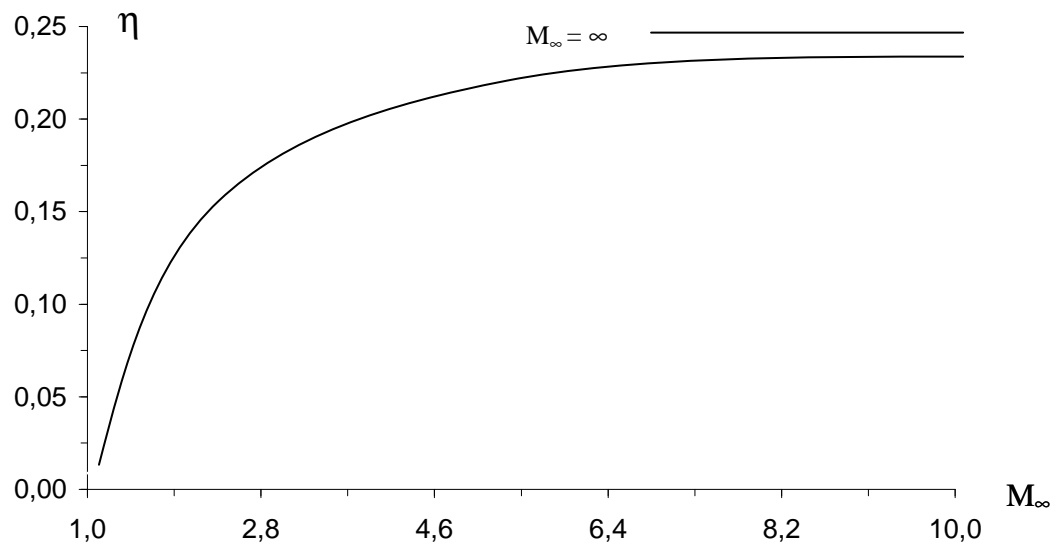


Fig.12. Dependence of the upper limit efficiency on the flight Mach number.